Sand Impact Tests of a Half-Scale Crew Module Boilerplate Test Article

Gregory J. Vassilakos[1] and Robin C. Hardy[2]

[1]Analytical Services & Materials, NASA Langley Research Center, Mail Stop 230, Hampton, VA 23681, Ph (757) 864-5278, email: gregory.j.vassilakos@nasa.gov
[2]Robin C. Hardy, NASA Langley Research Center, Mail Stop 495, Hampton, VA 23681, Ph (757) 864-6535, email: robin.c.hardy@nasa.gov

ABSTRACT

Although the Orion Multi-Purpose Crew Vehicle (MPCV) is being designed primarily for water landings, a further investigation of launch abort scenarios reveals the possibility of an onshore landing at Kennedy Space Center (KSC). To gather data for correlation against simulations of beach landing impacts, a series of sand impact tests were conducted at NASA Langley Research Center (LaRC). Both vertical drop tests and swing tests with combined vertical and horizontal velocity were performed onto beds of common construction-grade sand using a geometrically scaled crew module boilerplate test article. The tests were simulated using the explicit, nonlinear, transient dynamic finite element code LS-DYNA. The material models for the sand utilized in the simulations were based on tests of sand specimens. Although the LS-DYNA models provided reasonable predictions for peak accelerations, they were not always able to track the response through the duration of the impact. Further improvements to the material model used for the sand were identified based on results from the sand specimen tests.

INTRODUCTION

The Orion Multi-Purpose Crew Vehicle (MPCV) is being designed for water landing similar to Apollo. There does exist a small probability that the Orion MPCV could land onshore at NASA Kennedy Space Center (KSC) following a launch abort. A test series was undertaken at NASA Langley Research Center (LaRC) to obtain test data for the verification and validation of sand impact simulations performed using the explicit, nonlinear, transient dynamic finite element code LS-DYNA (LSTC 2007). This paper will present comparisons between test and simulation data for impacts of a half-scale boilerplate test article on beds of sand similar to the sand at KSC. Proposed improvements to the sand material model will also be presented.

SAND TYPES

Three different KSC sands were identified and evaluated (Thomas 2008 and 2009). These are Low Density Dry Sand (LDDS) from the dune area, High Density Flooded

Sand (HDFS) from the surf zone, and High Density In-Situ Moisture Sand (HDISMS) from the vegetated area inland of the dunes. The sand of primary interest is HDISMS as it is distributed over the greatest area.

The critical parameters that determine the mechanical properties of sand are the grain size distribution, the density, and the moisture content. The density can be adjusted to some extent through the use of a mechanical vibrator and the moisture can be adjusted by adding water. This leaves the grain size distribution as the most critical parameter to match when identifying sand that has properties similar to the KSC sands. Of the available commercial sands, Mason Sand from Yorktown Materials of Yorktown, VA was found to be closest to the KSC sands in grain size distribution. In this report, a particular condition of Yorktown Mason Sand is identified following the format YMS 100/5, which in this particular case corresponds to 100 lb/ft^3 dry density and 5% moisture. The ranges for the densities and moisture contents from laboratory measurements of the Yorktown Mason Sand as well as each of the KSC sands are shown in Table 1. The grain size distributions are shown in Figure 1.

Table 1. Moisture Content and Density for KSC Sands.

Sand	Moisture Content (%)	Wet Density (lb/ft^3)	Dry Density (lb/ft^3)	Porosity (%)
LDDS	2.70 – 3.05	80	77.49 – 77.84	53.3 – 53.4
HDFS	11.12 – 16.59 (~31 Pre-Test)	97.33 – 104.4	84.46 – 85.97	44.2 – 49.6
HDISMS	15.69 – 18.37	100.3	84.43 – 86.42	48.0 – 49.2
YMS	3.4 – 9.0	98.0 – 105.2	94.9 – 100.7	-

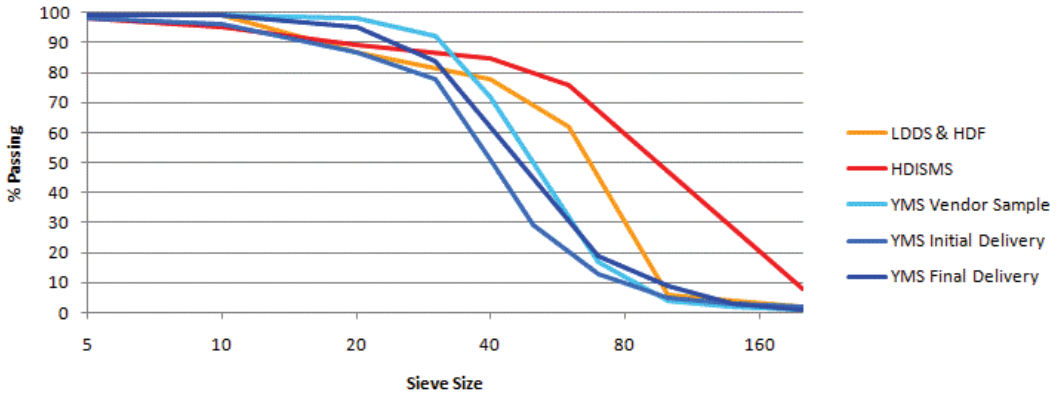

Figure 1. Grain Size Distribution.

SAND MATERIAL MODEL

The material model used in the LS-DYNA simulations was *MAT_SOIL_AND_FOAM (*MAT_005) (LSTC 2007). The material model

features a single value for the shear modulus, a single value for the unloading bulk modulus, and up to ten points defining the pressure versus volumetric strain relationship during loading. The yield stress in compression is treated as a quadratic function of the pressure. The quadratic function is defined via three input coefficients. The yield stress is compared against the von Mises stress to judge whether yielding has occurred. A tensile pressure cutoff is defined for yielding in tension.

The stress state of the material is determined by separating the strain into a pressure component and a deviatoric component. The pressure component of the stress is computed based on the pressure versus volumetric strain relationship. The deviatoric component of the stress is computed based on the shear modulus. The use of a single value for the shear modulus raises issues regarding the adequacy of the material model for determining the deviatoric stress. The nonlinear pressure versus volumetric strain relationship results in a nonlinear bulk modulus. A nonlinear bulk modulus coupled with a constant shear modulus results in a nonlinear Poisson's ratio. It is possible that the resulting Poisson's ratio could be nonphysical.

Specimen tests were performed to develop the coefficients of the material models (Thomas 2007 and 2008). The test set-up used to develop the sand models featured a specimen wrapped in a light membrane inside a pressure vessel with a piston acting on the top. A gage monitored the radial deformation. For the uniaxial strain tests, a feedback loop adjusted the pressure inside the pressure vessel to keep the radial deformation zero as the piston pressed down on top of the specimen. In these tests, the application of the loads was slow and water was allowed to drain from the specimens. As a consequence, there was no strain rate effect and the contribution to the bulk modulus from the water was lost. During an actual impact event, the strain rate would be high and the event would occur too quickly for the water to migrate out of the impact region. As a consequence, it is believed that the soil models represent lower bounds for the stiffness of the sand during an impact event.

Initial test simulations performed using the material models compared poorly with test data. This led to a series of studies of parameters that might influence the agreement between simulation and test, including the mesh density, contact surface definition, and material coefficients. It was found that simulations of the uniaxial strain tests were unable to duplicate the uniaxial strain test results (Schwer 2009). A modified material model was developed that provided much better agreement between the uniaxial strain test data and simulations. The slope of the pressure versus volumetric strain curve at 35 psi was used to define the shear modulus. The value of 35 psi avoids the highly nonlinear low pressure region of the curve while still being a relatively low pressure compared to the pressure peaks seen in the initial contact area of the impacts. In order to ensure that an unreasonably low or negative value for the Poisson's ratio did not result, the points below 35 psi were dropped from the pressure versus volumetric strain curve.

A simulation of the uniaxial strain tests for YMS 97/4 is shown in Figures 2 for the original and modified material models. Agreement between the tests and the modified material model is not perfect, but is greatly improved over the original material model.

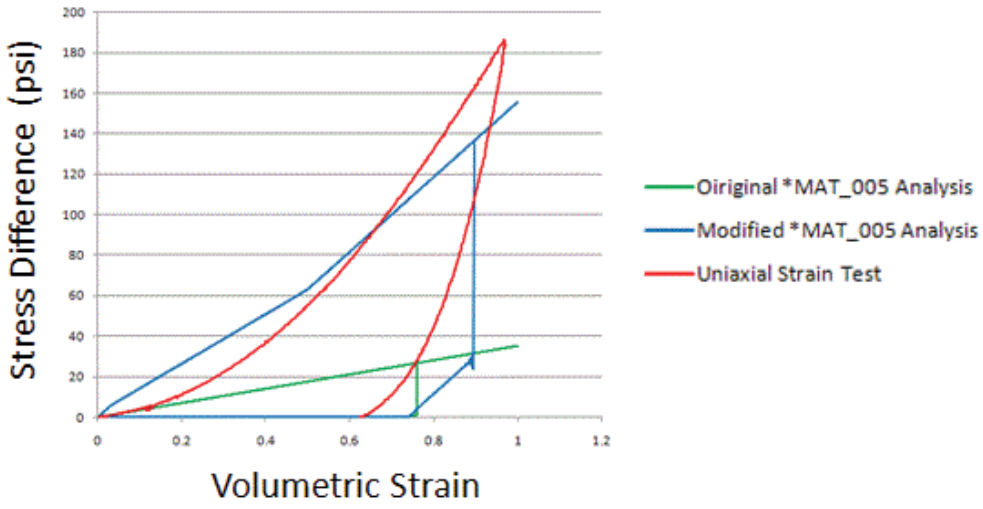

Figure 2. Uniaxial Strain Test Simulations for YMS 97/4.

HALF-SCALE BOILERPLATE TEST ARTICLE

The half-scale boilerplate test article is geometrically similar to the Orion MPCV. The boilerplate test article is 63 inches tall and 96 inches in diameter. The main area of the shell that represents the heat shield is a portion of a spherical surface with a radius of 120.75 inches. All structure is mild steel and is designed to be sufficiently robust to survive the impacts without permanent deformation. As a consequence, the boilerplate test article is approximately twice the weight of a true half-scale Orion MPCV.

During the tests, the boilerplate test article carried an onboard data acquisition system recording 25 channels of data. The instrumentation included accelerometers and rotation rate sensors. The motions were tracked with a conventional photogrammetry system that uses a single camera to record 2-D planar motion. The motions were also tracked with PONTOS (GOM 2011, Littell 2010), which uses two cameras to record 3-D motion. The following parameters were used to compare test and simulation results.

1. Acceleration histories at the CG.
2. Acceleration histories at the forward rim of the heat shield.
3. Pitch angle histories.
4. Crater depths.

The pitch angle was evaluated using data from both 2-D photogrammetry and 3-D PONTOS systems. Measurements from the 2-D and 3-D systems were in close agreement. The crater depth for the tests was measured by placing an aluminum flat bar across the crater and measuring the maximum distance from the bar to the bottom of the crater. The measurement did not include the height of the berm of plowed up material that existed at the forward end of the crater. The crater depth for the

analyses was recorded as the maximum excursion below the top surface of the sand for the node at the knuckle in the heat shield at the forward centerline.

The tests were conducted at the NASA LaRC Landing Impact Research (LandIR) facility, also known as the gantry. Vertical drop tests were performed under the 70-foot drop tower at the west end of the gantry. Swing tests were performed under the main spans of the gantry. The set-ups for the two types of tests are illustrated in Figures 3 and 4. The sand bed for the vertical drop test was approximately 20 feet wide, 20 feet long, and 4 feet deep. The sand bed for the swing tests was approximately 20 feet wide, 78 feet long, and 4 feet deep. The impact location for the vertical drop tests was approximately at the center of the sand bed. The impact location for the swing tests varied along the length of the sand bed as a function of the swing cable arrangement required to achieve the desired horizontal velocity.

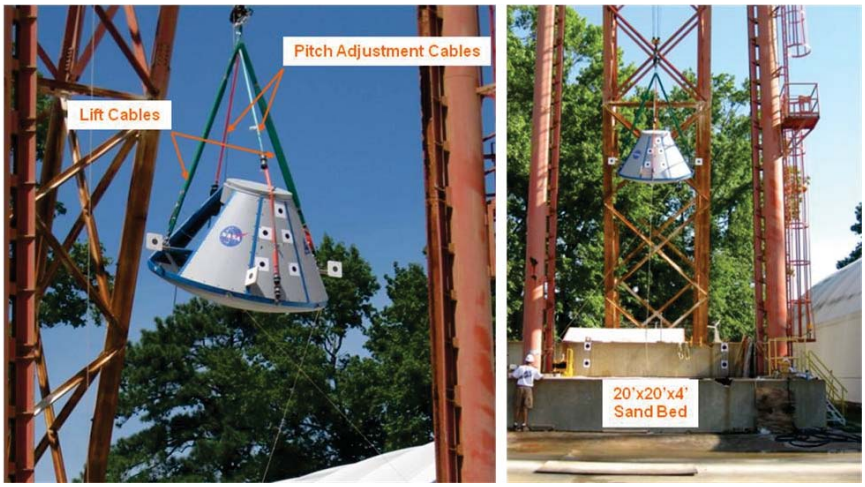

Figure 3. Vertical Drop Test Set-Up.

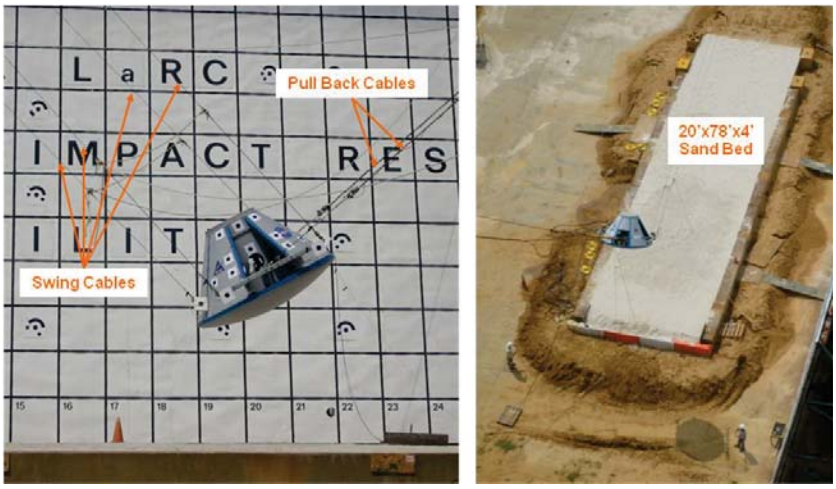

Figure 4. Swing Test Set-Up.

An attempt was made to control the density of the sand bed by building it in six-inch layers. Each layer was mechanically tamped before the next layer was added. The moisture level of the sand varied as a consequence of variations in humidity and rainfall. Soaker hoses were used to artificially raise the moisture level for some tests. Soil conditions were measured using a nuclear densitometer at an array of locations on the sand bed before and after each test. The soil moisture content varied from 3.4% to 9.0 % and the density varied from 94.9 lb/ft^3 to 100.7 lb/ft^3.

Twelve vertical drop tests and three swing tests were performed. For the vertical drop tests, the tests were performed with pitch angles of 23°, 28°, and 33°, and vertical velocities of 25 ft/sec and 35 ft/sec. For all the swing tests, the pitch angle was 28°. Two swing tests were performed with a vertical velocity of 25 ft/sec and a horizontal velocity of 30 ft/sec. The third swing test was performed with a vertical velocity of 35 ft/sec and a horizontal velocity of 38 ft/sec.

LS-DYNA SIMULATIONS

The majority of the dry density and moisture conditions measured during the tests were bracketed by three of the four YMS models for which the material coefficients had been determined. These three models. YMS 100/5, YMS 97/4, and YMS 96/8, were used to define a plane for each parameter of the material model on which the coefficient could be interpolated or extrapolated based on the measured soil density and moisture content.

The sand was modeled with both Lagrangian and Arbitrary Langrangian-Eulerian (ALE) meshes. In Lagrangian meshes, the nodes move and the elements deform with the material. In an ALE mesh, the mesh moves with the material at each time step, but is advected back to the original configuration between time steps, with the result that the material is treated as having moved through the mesh. The typical element size was 1 inch for the boilerplate test article and varied between 1 and 2 inches for the sand. For most of the simulations, the boilerplate test article was treated as rigid. A flexural version of the model was used for a limited number of simulations to confirm the validity of treating the boilerplate test article as rigid.

LS-DYNA uses a penalty method for contact in which a contact stiffness is defined that relates the penetration distance of one part into another to a contact pressure. For both the Lagrangian and ALE simulations, the default contact stiffness was used with the exception that for the Lagrangian simulations the "SOFT" algorithm was invoked, which is designed to handle the case of contacting parts that have elastic moduli that differ by orders of magnitude. The coefficient of friction between the boilerplate test article and the sand was set to 0.4.

For the vertical drop tests, the initial impact occurred at the forward rim. The boilerplate test article then rotated while rebounding backward. The boilerplate test article then rocked forward again. The final position was aft of the initial impact position. The motion sequence was similar for all the vertical drop tests and was closely matched by the simulations.

The motion sequence for the first swing test (ST01) is illustrated in Figure 5. Initial impact occurred at the forward rim. The boilerplate test article then rapidly rotated while sliding forward. The boilerplate test article did not dig deeply into the sand. In

its final position, the boilerplate test article was pitched slightly aft with the heat shield rim above the surface of the sand. The motion sequence was similar for all three swing tests. Neither the Lagrangian nor the ALE simulations were able to match the late time response of the swing tests.

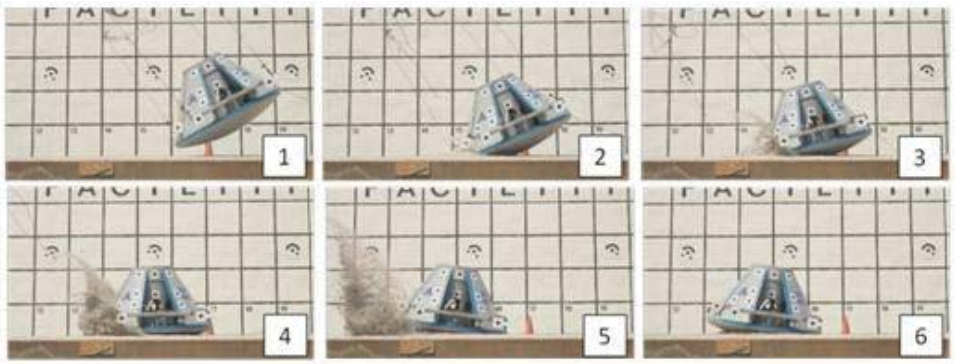

Figure 5. Motion Sequence for ST01.

For all swing test simulations, the boilerplate test article came to a stop with the forward rim below the surface of the sand. The simulation responses for the Lagrangian and ALE variants of ST01 are illustrated in Figure 6.

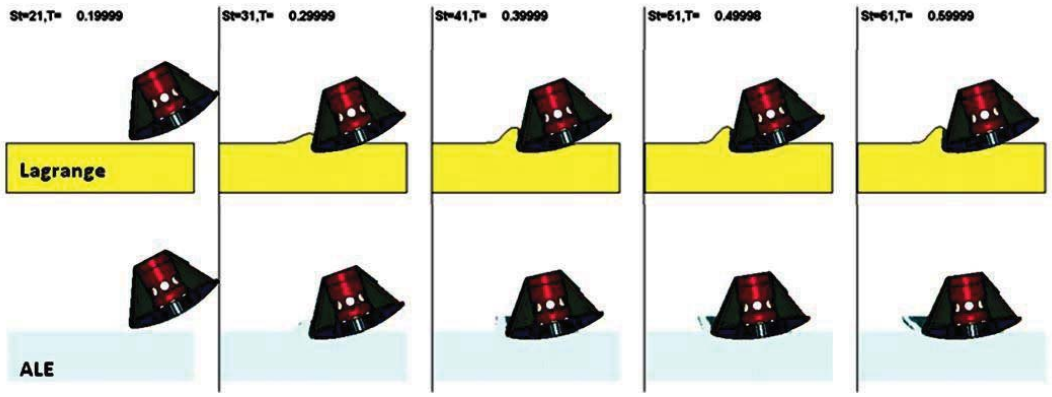

Figure 6. Responses of Lagrangian and ALE Variants of ST01 Simulation.

For the comparison of test and simulation time histories, the effect that gravity has on the accelerometer reading must be taken into account. Accelerometers measure force and interpret it as acceleration. While at rest, an accelerometer oriented vertically will measure a 1g force; however, the signal from the accelerometer is typically adjusted to record zero acceleration, effectively removing the effects of gravity. If an accelerometer is zeroed while in an upright position, the accelerometer will read 1g when turned on its side. As a consequence, corrections must be made when comparing test accelerometer data to simulation acceleration data. For simplicity, the acceleration histories from the simulations were adjusted to include the effects of gravity rather than removing the effects of gravity from the accelerometer data from the tests. Both the test and simulation acceleration data were filtered using a 60-Hz

Butterworth filter. Comparisons of the acceleration histories at the CG and the rim of the heat shield for test ST01 are shown in Figure 7. Charts showing the peak accelerations for all the tests are shown in Figure 8. Impact occurs 0.2 seconds after the start of the simulation. The first 0.2 seconds are used to ramp gravity to 1g.

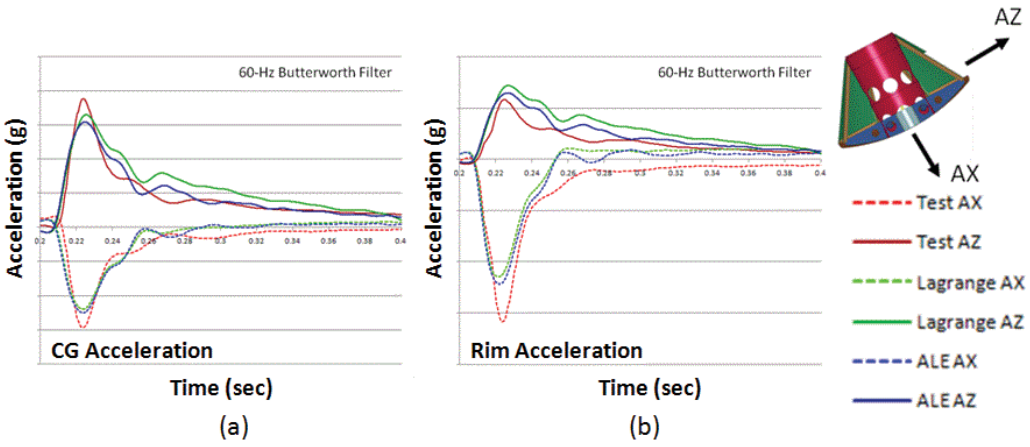

Figure 7. ST01 Acceleration Histories.

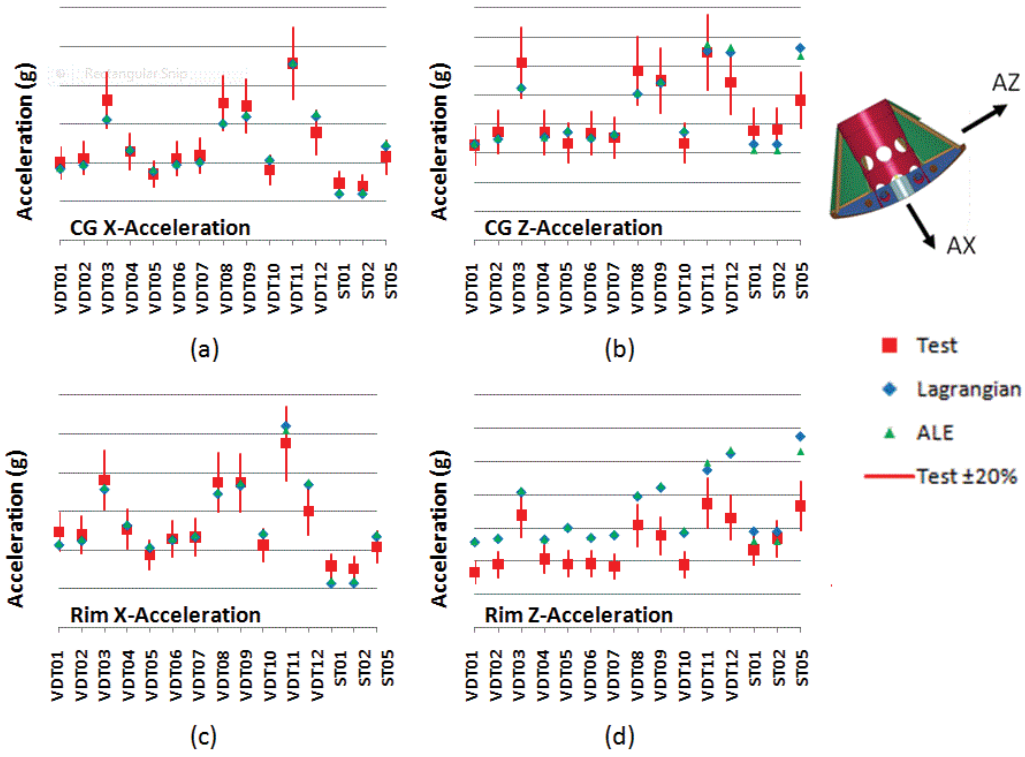

Figure 8. Peak Accelerations.

The results show that the Lagrangian and ALE solutions were generally in close agreement despite the severe deformation of the elements in the sand bed of the Lagrangian meshes. The peak accelerations at the CG from the simulations agreed

within 20% with the peak accelerations at the CG from the tests. The agreement for the peak X-Accelerations at the rim was also within 20% for most tests. On the other hand, the simulation results for Z-accelerations at the rim were consistently higher than for the tests.

The pitch angle time history for ST01 is illustrated in Figure 9. The Lagrangian and ALE solutions both diverged from the test data starting at approximately 0.1 seconds after impact. The ALE simulations did a better job of matching the test data for the pitch angle than the Lagrangian simulations. This may be in part due to the limited ability of a Lagrangian mesh to accommodate the severe element distortions resulting from the large deformations.

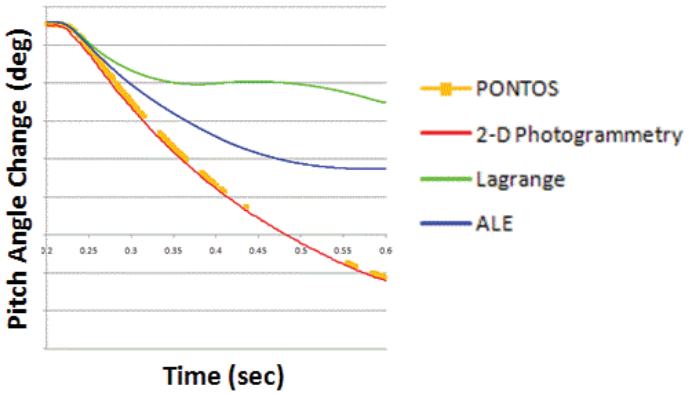

Figure 9. ST01 Pitch Angle History during First 0.4 Seconds Following Impact.

A chart illustrating the pitch angle change for all the tests during the first 0.4 seconds following impact is provided in Figure 10a. The pitch angle changes from the simulations were consistently higher than the tests for the vertical drop tests. The converse was true for the swing tests.

For most vertical and swing tests, the crater depth measurements agreed within 20%. VDT11 and ST05 were notable exceptions. That the agreement between the tests and simulations was reasonable was a surprise as the crater depth measurement for the test was performed well after the test and included soil spring back. The measurement for the simulation was the greatest depth the boilerplate test article penetrated into the sand and did not include spring back. The test and simulation crater depths are compared in Figure 10b.

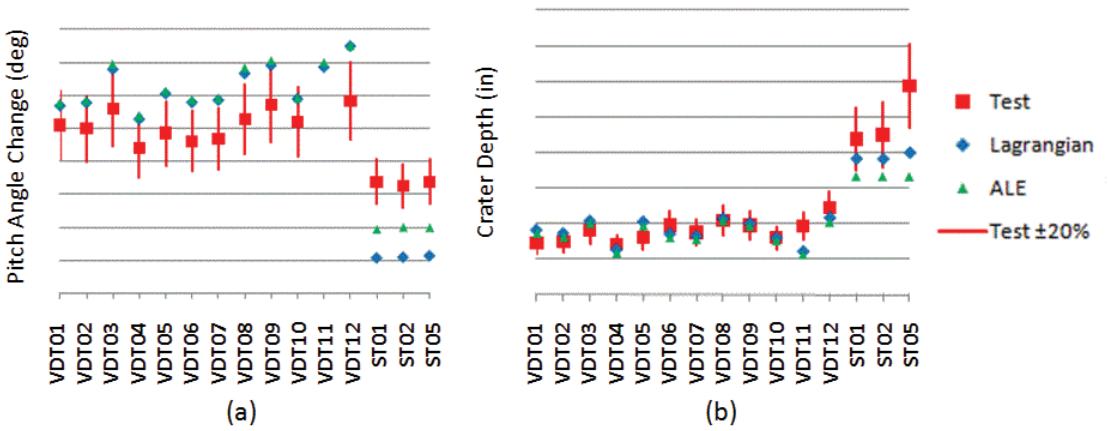

Figure 10. Pitch Angle Change during First 0.4 Seconds Following Impact and Crater Depths

PROPOSED IMPROVEMENTS TO LS-DYNA MATERIAL MODEL

The *MAT_SOIL_AND_FOAM (*MAT_005) material model features a curve for pressure versus volumetric strain, which produces a variable bulk modulus. When combined with a constant shear modulus, the analytical model produces a Poisson's ratio that varies as a function of pressure. Test data from uniaxial strain tests was used to compute a Poisson's ratio based on the ratio of the radial stress to axial stress (Thomas 2008 and 2009). The uniaxial strain test data shows that the Poisson's ratio is approximately constant. A plot generated for one of the sands (YMS 97/4) is provided in Figure 11.

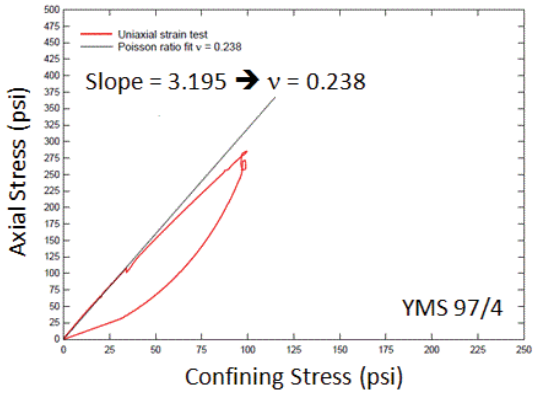

Figure 11. Poisson's Ratio Curve Fit for YMS 97/4

LS-DYNA has provision for user supplied subroutines to define material models for *MAT_041 through *MAT_050. For a material model more representative of the behavior demonstrated in the uniaxial test data, it is proposed that a Poisson's ratio that is independent of pressure be defined in LS-DYNA. The Poisson's ratio would

be used in conjunction with the pressure versus volumetric strain curve to define a shear modulus that is a function of pressure. At this time, this approach remains theoretical and has not been implemented.

CONCLUSIONS

The test series demonstrated that the LaRC LandIR facility can be used very effectively in conjunction with beds of construction-grade sand to simulate land landing impacts. The experience with the sand beds demonstrated that it was readily possible to measure the sand density and moisture content in situ; however, it was not possible to change the density and moisture content beyond a relatively narrow range. The principle findings from the simulations were that LS-DYNA simulations using the existing *MAT_005 material model did a reasonable job of predicting the early-time acceleration response provided that care was taken to properly define the material coefficents within the range of pressures of the sand impact. Simulations of the sand specimen tests used to generate the *MAT_005 material coefficients were effective in identifying changes to the coefficients needed to improve the accuracy of the simulation predictions. Improvement to the *MAT_005 material model may be possible by incorporating a constant Poisson's ratio rather than a constant shear modulus.

REFERENCES

Annett, M.S., "Evaluation of Orion Land Landing Passive Attenuation Methodologies with Subscale Testing and Analysis," NASA, Orion Landing System Advanced Development Project, Document No. LS-0059, February 20, 2009.

GOM mbH, "PONTOS – Dynamic 3D Analysis," Web, 2011, <http://www.gom.com/metrology-systems/3d-motion-analysis.html>.

Littell, J.D.: "Large Field Photogrammetry Techniques in Aircraft and Spacecraft Impact Testing," Society of Experimental Mechanics 2010 Annual Conference Proceedings. Indianapolis, Indiana. June 7-10, 2010. In Pub.

LSTC, "LS-DYNA^{TM} Keyword User's Manual, Version 971," Livermore Software Technology Corporation, May 2007.

Schwer, L.: Private Communications, Schwer Engineering & Consulting Services, 2009.

Thomas, M.A., Chitty, D.E., Gildea, M.L., and T'Kindt, C.M.: "Constitutive Soil Properties for Unwashed Sand and Kennedy Space Center," NASA/CR-2008-215334, Applied Research Associates, Inc., July 2008.

Thomas, M.A. and Chitty, D.E.: "Constitutive Soil Properties for Mason Sand and Kennedy Space Center," NASA/CR-2009-000000, Applied Research Associates, August 2009. In Pub.